EurJIC
European Journal of Inorganic Chemistry

Research Article
doi.org/10.1002/ejic.202300338

Chemistry Europe
European Chemical Societies Publishing

www.eurjic.org

Special Collection

On the Brink of Decomposition: Controlled Oxidation of a Substituted Arsanylborane as a Way to Labile Group 13-15-16 Compounds

Felix Lehnfeld,[a] Michael Seidl,[b] Alexey Y. Timoshkin,[c] and Manfred Scheer*[a]

The reactivity of the organic-substituted arsanylborane $tBuAsHBH_2NMe_3$ (**1**) towards different elemental chalcogenes as well as organic oxidants such as O-NMe_3, Me_3Si–O–O-$SiMe_3$, MesCNO and cyclohexenesulfide is reported. By the reaction of **1** with grey selenium, the selenium oxidation product $tBuAs(Se)HBH_2NMe_3$ (**2**) was obtained. For the oxidation with sulfur, the two products $tBuAs(S)HBH_2NMe_3$ (**3a**) and $tBuAs(S)SHBH_2NMe_3$ (**3b**) could be isolated as oils. The structural characterization of $As(tBuAs(S)SHBH_2NMe_3)_3$ (**4**) as well as corresponding DFT computations allow insights into the decomposition behavior of **3a** and **3b** in solution. For the reaction of MesCNO with **1**, the formation of an unusual As–H activation product Mes-C(NOH)-AstBu-BH_2NMe_3 (**5**) is observed. In the reaction with Me_3N–O, the first isolatable oxo-arsanylboranes $tBuAs(O)HBH_2NMe_3$ (**6a**) and $tBuAs(O)OHBH_2NMe_3$ (**6b**) are obtained, with **6b** also being accessible via the controlled reaction of **1** with air.

Introduction

In recent years, the investigation of mixed main group element compounds has been of great interest due to their increasing number of applications. Binary group 13–15 compounds are for instance used as materials for micro- and nanoelectronics, in light emitting diodes, photodetectors and in semiconductors.[1] Therefore, suitable precursors, e.g. for chemical vapor deposition, have been heavily researched over the last decades.[2] Moreover, saturated adducts such as ammonia borane are a well investigated class of monomeric compounds,[3] useful as potential hydrogen storage materials[4] and as starting materials in dehydrocoupling reactions.[5] A similar reactivity has been reported for the heavier homologs, the phosphane-borane adducts.[3a,c,6]

With respect to a potential application in semiconductors, the reactivity of group 13/15 compounds towards chalcogens is of interest, especially when considering the importance of selenium and tellurium in semiconductor applications.[7] When only looking at group 15 elements, there are many examples of phosphorus-chalcogen-containing compounds as important reagents in organic synthesis, usually achieved via oxidation with elemental chalcogens or organic oxidants.[8] Important examples include e.g. Lawesson's reagent[9] and Woolins' reagent.[10] Moreover, organophosphorus-chalcogen compounds are used in a broad variety of applications such as pesticides, as precursors for metal-chalcogenide containing thin films or nanoparticles and as lubricant additives.[11]

As for the oxidation chemistry of phosphino-borane adducts or phosphinoboranes, only limited studies have been performed so far. Known examples include boranylphosphines oxides and sulfides as well as some very rare selenide and telluride derivatives (Scheme 1, **I**–**II**).[12]

To deepen the understanding of this topic, our group has great interest in the oxidation of pnictogenylboranes of the type $RR'EBH_2NMe_3$ (E = P, As; R = H, *t*Bu, Ph; R' = H, *t*Bu, Ph). We were able to report about the oxidation of the parent phosphanylborane as well as substituted derivatives in recent years.[13] However, when looking at the heavier homolog, only little is known about arsenic chalcogen compounds: In addition to rather well investigated arsine-oxides,[14] a limited number of arsine sulfides and selenides (Scheme 1, **III**–**IV**) is known.[15] Furthermore, we were able to report the oxidation of $Ph_2AsBH_2NMe_3$ with chalcogens (Scheme 1, **V**) not long since.[16] However, regardless of many attempts, isolating an arsanylborane oxide is still an open topic. Having recently reported the relatively stable although reactive substituted arsanylborane $tBuAsHBH_2NMe_3$ (**1**),[17] the question arose if this compound can

[a] Dr. F. Lehnfeld, Prof. Dr. M. Scheer
Institut für Anorganische Chemie, Universität Regensburg
93040 Regensburg (Germany)
E-mail: manfred.scheer@ur.de
Homepage: www.uni-regensburg.de/chemie-pharmazie/anorganische-chemie-Scheer

[b] Dr. M. Seidl
Institute for General, Inorganic and Theoretical Chemistry
Leopold Franzens-Universität Innsbruck
Innrain 80/82, L.01.070
6020 Innsbruck, Austria

[c] Prof. Dr. A. Y. Timoshkin
Institute of Chemistry, St. Petersburg State University
Sankt-Peterburg, 199034 Universitetskaya emb. 7/9, St. Petersburg (Russia)

Supporting information for this article is available on the WWW under https://doi.org/10.1002/ejic.202300338

Special Collection Part of the celebratory collection for Rainer Streubel.

Research Article
doi.org/10.1002/ejic.202300338

Chemistry Europe
European Chemical Societies Publishing

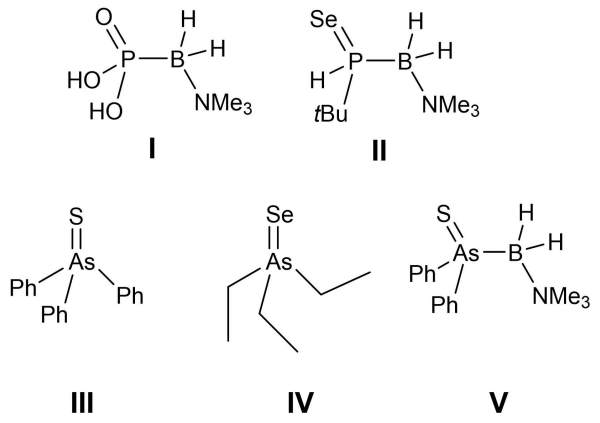

Scheme 1. Selected examples of chalcogenated pnictogenylboranes (**I**, **II**, **V**) and organic arsenic chalcogenides (**III**, **IV**).

be used as starting material for oxidation reactions. This is of importance since the oxidation reactions of the corresponding phosphorus derivative *t*BuPHBH$_2$NMe$_3$ was studied. Herein, we report on the results of the controlled oxidation of **1** using various chalcogens and organic oxidants. Moreover, the formation of the first ever isolatable oxo-arsanylborane is reported.

Results and Discussion

Reactivity towards selenium

As previous reactions with similar compounds have revealed the reactivity of the oxidizing agent to be the key for controlling the reaction, as unwanted side products and decomposition need to be reduced to a minimum. Firstly, the reactivity of the weaker oxidants selenium and tellurium towards **1** was investigated. Neither elemental tellurium nor Et$_3$P–Te showed any reactivity towards **1** at room temperature or elevated temperatures, which could additionally be supported by DFT calculations revealing the corresponding reaction to be endergonic by 2.8 (Et$_3$PTe) or 6.6 (Te) kJ/mol, respectively. Grey selenium, however, did reveal a rather controlled reactivity. After stirring a stochiometric mixture of grey selenium and **1** for 3 h in toluene at −30 °C while slowly increasing the temperature to r.t., the complete dissolution of selenium and a color change from colorless to yellow could be observed (Scheme 2).

After workup, compound **2** could be isolated as a yellow oil in good yields. By storing a saturated solution of **2** in toluene at

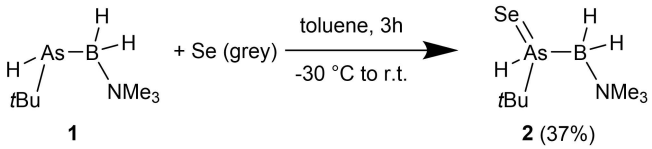

Scheme 2. Reaction of **1** with one equivalent of grey selenium.

−30 °C, crystals of **2** suitable for X-ray diffraction analysis were obtained (Figure 1) with a crystalline yield of 37 %.

The isolated product *t*BuAs(Se)HBH$_2$NMe$_3$ (**2**) was characterized by multinuclear NMR spectroscopy. The ^{11}B{^{1}H} NMR spectrum of **2** reveals a broad singlet at $\delta = -3.9$ ppm, which shows further splitting with a $^1J_{B,H}$ of 109 Hz in the ^{11}B NMR spectrum. Exhibiting rapid decomposition in solution even at low temperatures, small signals of decomposition products are observed. In the ^{1}H NMR spectrum of **2**, the signals for the *t*Bu group at $\delta = 2.67$ ppm and for the As–H at $\delta = 2.34$ ppm are assigned, both of them shifted to lower field compared to **1**. The signal corresponding to the NMe$_3$ group at $\delta = 2.97$ ppm is in a similar range as for Ph$_2$As(Se)BH$_2$NMe$_3$.

The solid-state structure of **2** exhibits the structural motif of a B–As–Se chain, as has been observed for the diphenyl-substituted derivative Ph$_2$As(Se)BH$_2$NMe$_3$. The structural differences regarding the substitution pattern on the arsenic atom are small. The As–Se and As–B bonds with 2.2592(3) Å and 2.094(3) Å, respectively, are both in the expected range and slightly elongated compared to Ph$_2$As(Se)BH$_2$NMe$_3$. The bond angles around the arsenic atom reveal a distorted tetrahedral environment with a B–As–Se bond angle of 119.86(8)° and a B–As–C bond angle of 108.99(11)°. Due to the asymmetric substitution on the arsenic atom, two enantiomers are formed during the reaction. As a racemic mixture of **1** is used as starting material, also, both enantiomers are present in the unit cell as a racemic mixture, disordered at the same position in the solid state.

DFT calculations confirmed the exergonic nature of the reaction with one equivalent of selenium, which is favored by 21.3 kJ/mol. Although the reaction with two equivalents of selenium is favored by about 45.6 kJ/mol according to the computational data, experimental findings give no indication of a stable product being formed, regardless of the conditions applied. Most likely, this behavior is based in fast and energetically favored decomposition pathways in the presence of two equivalents of Se.

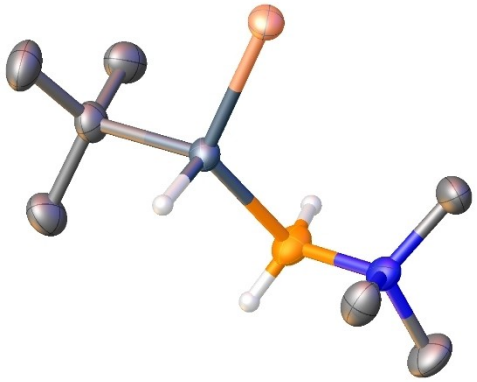

Figure 1. Molecular structure of **2**. Only the R enantiomer is depicted for clarity. Thermal ellipsoids displayed at 50 % probability. Selected bond distances [Å] and angles [°]: As–Se 2.2592(3), As–B 2.094(3), As–C 1.989(2), N–B 1.586(3); C–As–Se 110.17(7), C–As–B 108.99(11), B–As–Se 119.86(8).

Research Article
doi.org/10.1002/ejic.202300338

Reactivity towards sulfur

For the sulfurization reactions, two different reagents have been used. Whereas the reaction with cyclohexenesulfide only leads to an inseparable mixture of products accompanied by immediate decomposition (for further information: SI, section 3), the reaction with elemental sulfur leads to full conversion both for a 1:1 and a 1:2 stoichiometry accompanied by small amounts of decomposition products (Scheme 3). The compounds *t*BuAs(S)HBH$_2$NMe$_3$ (**3a**) and *t*BuAs(S)SHBH$_2$NMe$_3$ (**3b**) are obtained as yellow oils and characterized by multinuclear NMR spectroscopy, as no crystals suitable for X-ray diffraction analysis could be obtained. **3a** and **3b** both exhibit a broad singlet in the $^{11}B\{^1H\}$ NMR spectrum at $\delta = -0.7$ ppm and $\delta = -6.8$ ppm, respectively. Further splitting in the ^{11}B NMR with a similar $^1J_{B,H}$ of about 114 Hz is observed for both compounds. The ^1H NMR spectra of the two compounds reveal very similar signals for the *t*Bu group in the range of $\delta = 1.3$–1.1 ppm and for NMe$_3$ at ca. $\delta = 3$ ppm. The broadened and partly overlapped signal corresponding to the BH$_2$ moiety is observed in the region of $\delta = 2$–3 ppm.

For **3b**, a broad singlet for the S–H unit can be perceived at $\delta = 2.84$ ppm, whereas the spectrum of **3a** exhibits a signal at $\delta = 2.17$ ppm, which can be assigned to the As–H moiety. ESI-TOF mass spectra of **3a** and **3b** reveal peaks at m/z = 236 and m/z = 268 Da, respectively, which correspond to the release of H$_2$ from the compounds during the ionization process. After storing a solution of **3a** at −30 °C for a week, additional signals corresponding to **3b**, **1** and BH$_3$NMe$_3$ were observed in the ^{11}B NMR and mass spectra. This indicates an intermolecular sulfur transfer between two equivalents of **3a** in solution, which is besides accompanied by decomposition processes.

Both the formation of **3a** and **3b** were additionally investigated by DFT computations. In agreement with experimental findings, the reactions shown in Scheme 3 are both exergonic by 42.0 kJ/mol and 98.4 kJ/mol, respectively.

Regardless of numerous attempts to crystallize **3a** or **3b**, it was not possible to obtain crystals suitable for X-ray diffraction analysis. However, it was possible to isolate crystals of one of the decomposition products (Figure 2) after storing a saturated solution of **3a** for a week at −30 °C. Compound **4** crystallizes in the space group $P\bar{3}$ as colorless blocks and consists of three deprotonated moieties of **3b**, which are connected via a central threefold coordinated arsenic atom. The As–S bond lengths around the central arsenic atom are with 2.2822(13) Å in the range of As–S single bonds, slightly longer than the ones connected with the arsanylborane moiety with 2.2394(13) Å. They are both notably longer than the terminal As–S bonds present in the molecule with 2.1130(14) Å. This is in agreement with the more double bond character of these bonds and is comparable to the already known Ph$_2$As(S)BH$_2$NMe$_3$. The central arsenic atom reveals a trigonal pyramidal arrangement with symmetric S–As–S bond angles of about 92.54(5)°. All other bond angles and bond lengths are in the range of single bonds.

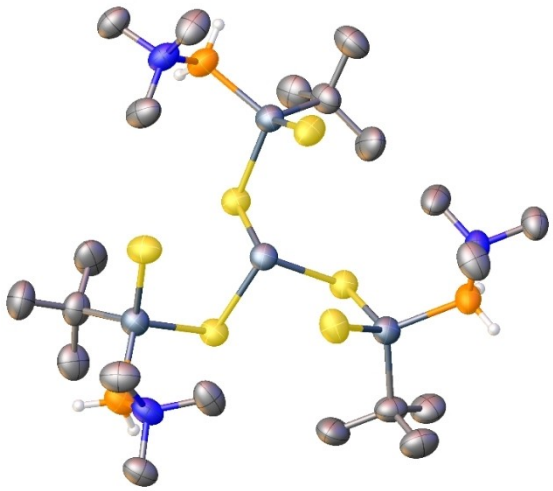

Figure 2. Molecular structure of **4** in the solid state. Solvent molecules in the unit cell are not depicted for clarity. Thermal ellipsoids displayed at 50% probability. Selected bond distances [Å] and angles [°]: As1-S1 2.2394(13), As1-S2 2.1130(14), As2-S1 2.2822(13), As1-C 1.987(5), As1-B 2.077(6), B–N 1.579(7); S1-As2-S1 92.54(5), S2-As1-S1 108.24(6), C–As1-S1 103.33(18), C–As1-S2 110.5(2), B–As1-S1 105.0(2), B–As1-S2 121.26(18), As1-S1-As2 99.52(5)

As the formation for **4** is not unambiguous, DFT calculations were applied to identify a potential pathway (Scheme 4). The proposed reaction is not only thermodynamically very favored, but also in good agreement with some experimental findings: **4** was crystallized from a solution of **3a**, so the already described transformation of **3a** to **3b** under elimination of **1** would yield the necessary starting materials for its synthesis. In addition, after several days, NMR data of **3a** solutions indicate a decomposition pathway involving the formation of BH$_3$NMe$_3$. Unfortunately, any attempts to synthesize **4** either from a 3:1 mixture of **3b** and **1** or by reproducing the conditions from the initial synthesis from a solution of **3a** have not been successful up to this point, although the decomposition of **3a** under formation of **3b** and **1** in solution could be reproduced. This is, however, not unexpected, as **4** represents an intermediate product occurring during the decomposition.

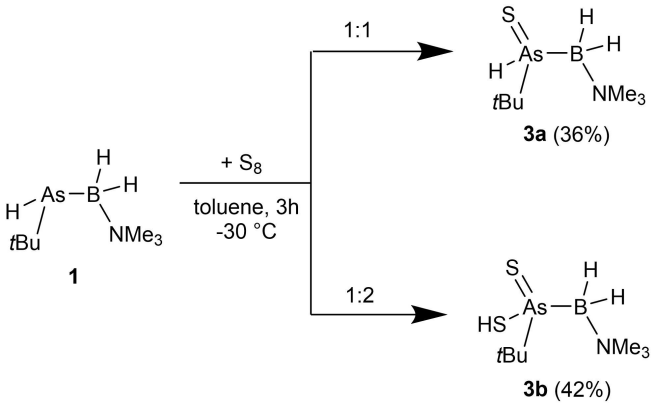

Scheme 3. Reaction of **1** with elemental sulfur.

Research Article
doi.org/10.1002/ejic.202300338

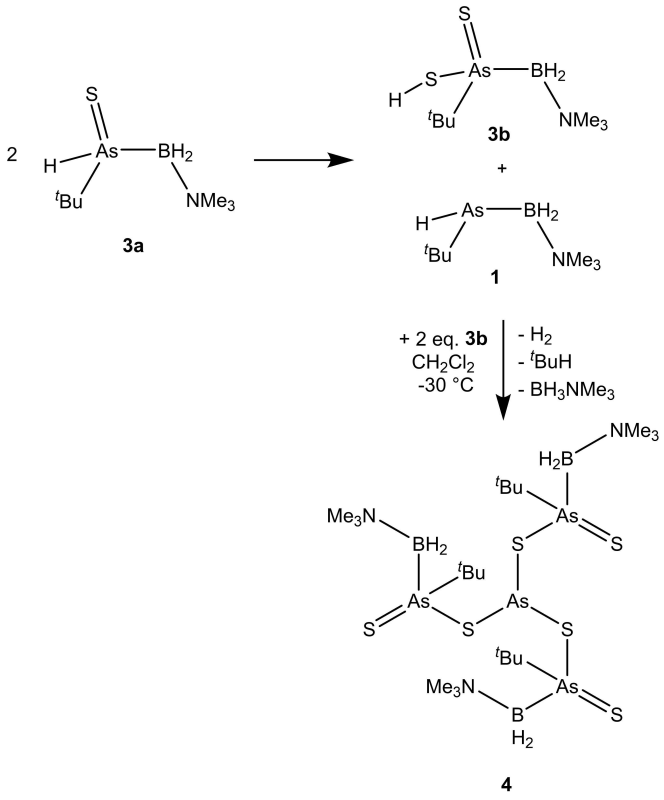

Scheme 4. Proposed formation of **4** from a solution of **3 a** as indicated by DFT calculations and experimental data.

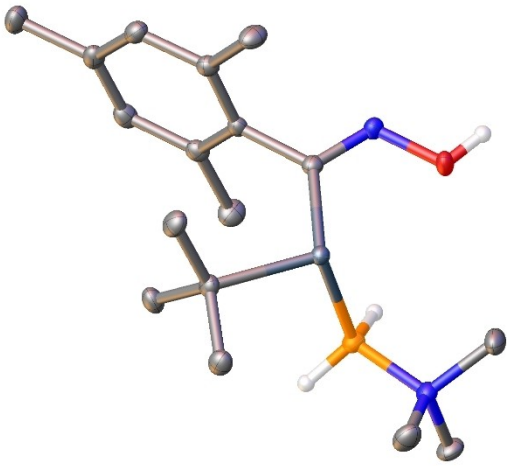

Figure 3. Molecular structure of **5** in the solid state. Thermal ellipsoids displayed at 50 % probability. Selected bond distances [Å] and angles [°]: As-C_{tBu} 2.0255(15), As-C_{CNO} 1.9799(15), As–B 2.1056(17), N–O 1.4218(16), N-C_{CNO} 1.281(2), B–N 1.625(2); C_{tBu}-As–B 103.25(7), C_{CNO}-As-C_{tBu} 106.43(6), C_{CNO}-As–B 98.98(6), C_{CNO}-N–O 113.36(12), N–B–As 110.61(10), C_{Mes}-C_{CNO}-As 124.53(10), N-C_{CNO}-As 121.59(11).

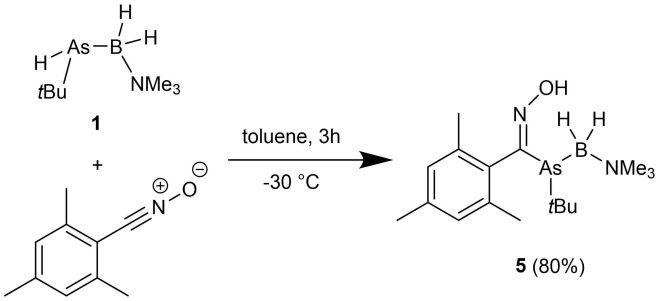

Scheme 5. Reaction of **1** with mesitylnitrile-N-oxide.

Reactivity towards oxygen sources

The formation of pnictogenylborane-oxo compounds was successful in the case of the phosphanylborane derivatives, but for both the parent arsanylborane $AsH_2BH_2NMe_3$ and the substituted $Ph_2AsBH_2NMe_3$ no oxo species could be isolated so far due to the rapid decomposition of the products.[16,18] In the case of the latter, the resulting species $Ph_2As(O)BH_2NMe_3$ could only be characterized in solution at low temperatures. To obtain an isolatable oxidation product for the *t*Bu derivative, four different oxidizing agents were applied. While successful for the oxidation of phosphanylboranes, $Me_3Si–O–O–SiMe_3$ did not lead to a controllable reaction with **1**, but only to inseparable product mixtures accompanied by insoluble decomposition products even at low temperatures.

When reacting one equivalent of MesCNO with **1** in toluene at −30 °C, a rapid formation of a white precipitate was observed. The thus obtained analytically pure powder, although very instable in solution, can be recrystallized to gain single crystals suitable for X-ray diffraction analysis. The solid-state structure of the product **5** (Figure 3) reveals not to be the arsanylborane oxide, but a product of a hydroarsination reaction of the nitriloxide group (Scheme 5).

In the solid-state structure of **5** (Figure 3), the newformed C–As bond is with 1.9799(15) Å in the range of a single bond. The arrangement around the originally sp-hybridized carbon atom at the N-oxide group changes to a distorted trigonal planar arrangement with a C–C–As bond angle of 124.53(10)° and an N–C–As bond angle of 121.59(11)°. Compared to MesCNO, the C–N bond is elongated with 1.281(2) Å, whereas the N–O bond is slightly shortened to 1.4218(16) Å. The bond length of this O–H group is in the expected range for a O–H single bond. This newformed –OH group allows the formation of hydrogen bonds and leads to the hydrogen-bridged dimer in the solid state.

DFT calculations have revealed that the formation of **5** is slightly endergonic with 20 kJ/mol, but due to the additional stabilization by dimerization, the formation is energetically favored.

Despite the very rapid decomposition of **5** in solution, it was possible to characterize **5** by multinuclear NMR spectroscopy by minimizing the time in solution before and during the measurements. In the $^{11}B\{^1H\}$ NMR spectrum, **5** reveals a singlet at $\delta = -2.5$ ppm, which, in the ^{11}B NMR spectrum, shows broadening without revealing a clear coupling pattern. In the ^1H NMR spectrum, in addition to the signals for the NMe_3 group at $\delta = 2.77$ ppm and the *t*Bu group at $\delta = 0.90$ ppm, especially the absence of an As–H signal with instead a broad singlet

Research Article
doi.org/10.1002/ejic.202300338

representing the O–H moiety at $\delta = 7.7$ ppm is noteworthy. The signal corresponding to the BH_2 group cannot be assigned due to being heavily overlapped by signals corresponding to the CH_3 groups of the mesityl group as well as the *t*Bu and the NMe_3 group. The ESI-TOF mass spectrum of **5** in CH_3CN shows a peak at m/z = 350 Da. This matches **5** to an $[M\text{-}OH]^+$ moiety which is formed during the ionization of **5** by the cleavage of H_2O initiated by the addition of H^+ during the ionization.

Since **5** was still not the desired oxo-arsanylborane, a different oxidizing agent was applied. Therefore, the reaction with one or two equivalents of trimethylamine-N-oxide was performed. For both cases, the reactivity of **1** towards the oxidizing agent is significantly lower than towards the previously used oxidizing agents. Nevertheless, full conversion to the two different oxidized compounds **6a** and **6b** was observed after 16 h at room temperature according to NMR spectroscopic monitoring of the reaction solution (Scheme 6). In contrast to the reaction with other oxidizing agents, these reactions are clean, and only if the compounds remain in solution for several days at room temperature, decomposition is observed.

In the $^{11}B\{^1H\}$ NMR spectrum of **6a**, a slight low field shift compared to **1** can be observed for the signal corresponding to the BH_2 group, revealing a singlet at $\delta = -0.4$ ppm. For **6b**, the singlet is observed at $\delta = -5.7$ ppm. Unfortunately, the formation of a 1:2 mixture of **6a** and **6b** could not be prevented so far despite applying various reaction conditions. As in the case of the reaction with sulfur, the transformation of **6a** to **6b** occurs under elimination of **1** accompanied by decomposition reactions. In the ^{11}B NMR spectrum for both compounds, further splitting into broad triplets with very similar $^1J_{B,H}$ coupling constants of ca. 115 Hz is observed.

Also, the ^1H NMR spectra of the two compounds reveal some similar features due to their similar chemical nature. Both show singlets for the NMe_3 and the *t*Bu groups in the ranges at $\delta = 2.7$ ppm and $\delta = 1.1$ ppm, respectively. In both cases, signals corresponding to the BH_2 can be observed in the range of $\delta =$ 2–3 ppm, but they are heavily broadened and superimposed. The most significant difference is the signal corresponding to the As–H group at $\delta = 1.73$ ppm in the spectrum for **6a**, which is replaced by a low field shifted and very broad signal for the OH-group at $\delta = 5.50$ ppm in the case of **6b**.

No crystals suitable for X-ray diffraction analysis could be obtained for **6a**, as either complete decomposition or transformation into **6b** and **1** take place during the crystallization process. Even though compound **6b** also reveals rapid decomposition in solution, it was possible to obtain single crystals suitable for X-ray diffraction analysis by storing a saturated solution in a 9:1 mixture of toluene and methanol at −30 °C (Figure 4).

6b crystallizes as colorless blocks in the space group $P2_1/c$. In the solid-state structure, two units of **6b** are stabilized by hydrogen bonds, arranged as a dimer. The As–B and As-*t*Bu bonds in **6b** are slightly elongated compared to **1**, but still in the range of a single bond. The newformed As–O bonds are in the expected ranges: With 1.683(16) Å, the terminal As–O bond is in the range of a double bond, whereas the bond to the OH group is longer with 1.7441(15) Å and therefore in the expected range of a single bond. The newformed O–H bond is rather short with 0.794(1) Å and therefore definitely a single bond, whereas the intermolecular interaction clearly represents a hydrogen bond with 1.775(3) Å. All other bond lengths are in the expected range.

For compound **6b** in solution, some unusual behavior was observed: In the ^1H NMR spectrum of freshly prepared and precipitated **6b**, an additional signal corresponding to about one equivalent of NMe_3 is observed, which cannot be removed by applying reduced pressure or washing the compound with apolar solvents. The mass spectrum of this precipitate in CH_3CN reveals a strong peak at m/z = 313 Da, which correlates with $[M + NMe_3]^+$. Therefore, it is likely that, in solution, after the formation of **6b**, adduct formation with one equivalent of NMe_3 takes place via a hydrogen bond to the -OH group of **6b**. However, this adduct could not be crystallized. By cleaving the NMe_3-adduct in the presence of methanol, **6b** could be obtained as colorless blocks in small yields, as **6b**, in the absence of an additional equivalent of

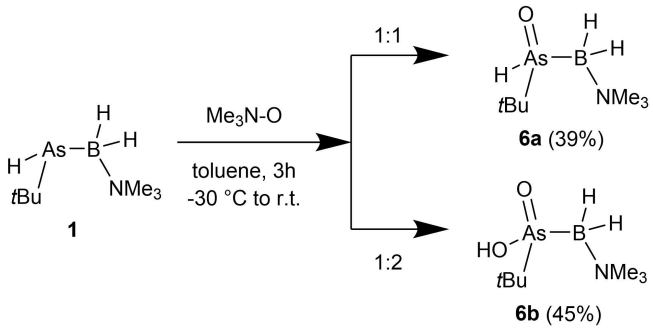

Scheme 6. Reaction of **1** with trimethylamine-N-oxide.

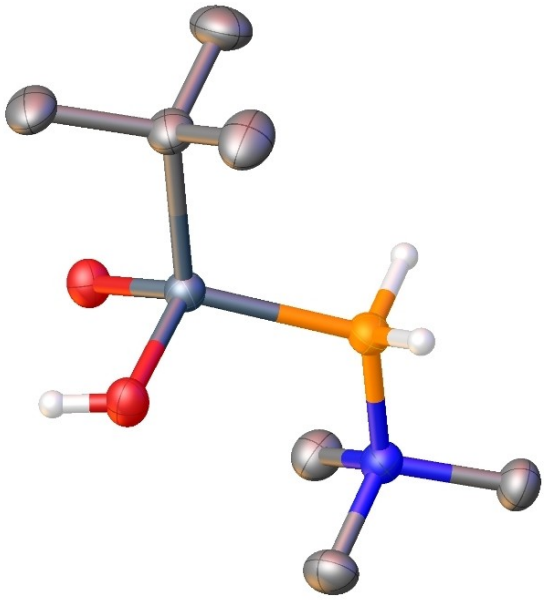

Figure 4. Molecular structure of **6b** in the solid state. Thermal ellipsoids displayed at 50% probability. Selected bond distances [Å] and angles [°]: As–O1 1.683(16), As–O2 1.7441(15), As–C 1.971(2), As–B 2.056(3), B–N 1.600(3); O1-As–O2 109.26(7), O1-As–C 107.39(9), O1-As–B 115.03(10), O2-As–C 103.81(9), O2-As–B 108.96(9), C–As–B 111.79(10), N–B–As 112.22(14).

Research Article
doi.org/10.1002/ejic.202300338

NMe_3, reveals dimerization in the solid state, leading to the successful crystallization of the compound.

Compound **6b** is also accessible by exposing compound **1** to a controlled amount of air. By opening a flask containing a 0.5 M solution of **1** in toluene for 30s without stirring, and then storing it at −30 °C for three days, a large number of colorless crystals of **6b** were isolated. X-ray diffraction analysis reveals that these temperature-sensitive crystals consist of **6b**, which forms additional hydrogen bonds to 0.7 to 1 equivalents of water (Figure 5). The interactions towards the H_2O molecules are, with a distance of 1.940(2) Å, longer than the hydrogen bonds that are responsible for the dimer formation. Overall, the arrangement of the dimeric units bridged by water forming a three-dimensional network in the solid state is observed (for X-ray structure and further information refer to SI).

DFT calculations on both the water-free **6b** as well as **6b x H_2O** have shown that in both cases the hydrogen bonds are essential for the stabilization for the compound in the solid state, stabilizing them by about 50 kJ/mol in the case of **6b** and 70 kJ/mol in the case of **6b x H_2O**. However, the experimental results show that even though the additional hydrogen bonds offered by the presence of water lead to thermodynamical stabilization, the further degradation by the cleavage of the As–B bond is heavily favored in the presence of water. Therefore, **6b x H_2O** is very instable at room temperature in solution and in the solid state according to experimental findings.

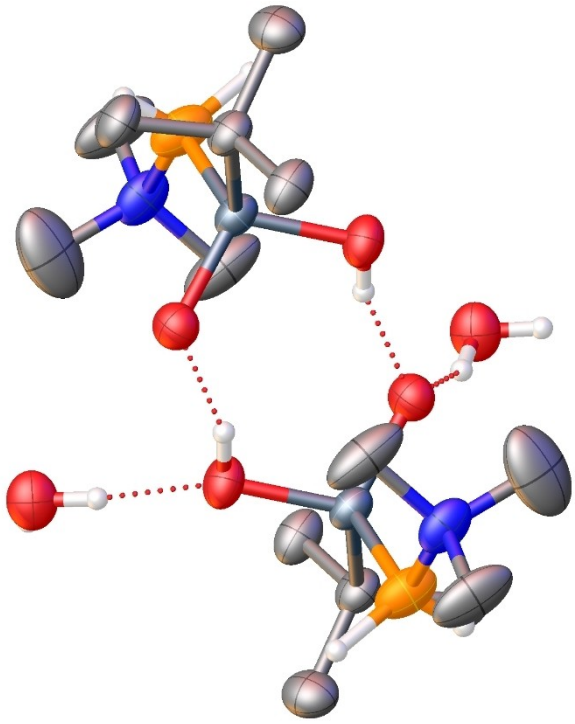

Figure 5. Molecular structure of a dimeric unit of **6b x H_2O** in the solid state. Thermal ellipsoids displayed at 50% probability. Selected bond distances [Å] and angles [°]: As–O1 1.706(2), As–O2 1.719(2), As–C 1.971(3), As–B 2.066(4), B–N 1.587(5); O1-As–O2 107.84(11), O1-As–C 105.44(11), O1-As–B 117.79(16), O2-As–C 104.14(11), O2-As–B 111.25(16), C–As–B 109.39(14), N–B–As 114.1(2).

Tautomerization of compounds 2, 3a and 6a

However, for compounds **2**, **3a** and **6a**, the products of the reaction with one equivalent of the respective chalcogen, a different isomer has to be considered (Scheme 7).

We also addressed the possibility of the isomerization of **2**, **3a** and **6a** into the corresponding tautomers by computations where the H–As=E group is replaced by an As–E–H group. Two isomerization pathways, mono- and bimolecular, were considered (Scheme 8, cf. SI for details). The reaction enthalpies and activation enthalpies for both pathways are summarized in Table 1.

The ^{t}BuAs(EH)BH_2NMe_3 tautomers are predicted to be more stable for all E, but the energy differences between the isomers decreases in the order O > S > Se. The activation barriers for the monomolecular isomerization are quite high (above 137 kJ mol^{-1}) and increase in the order Se < S < O (Table 1). Thus, it appears that a monomolecular hydrogen shift is kinetically hindered for all studied compounds.

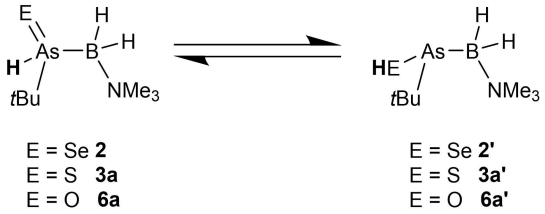

Scheme 7. Tautomerization of the compounds **2**, **3a** and **6a**.

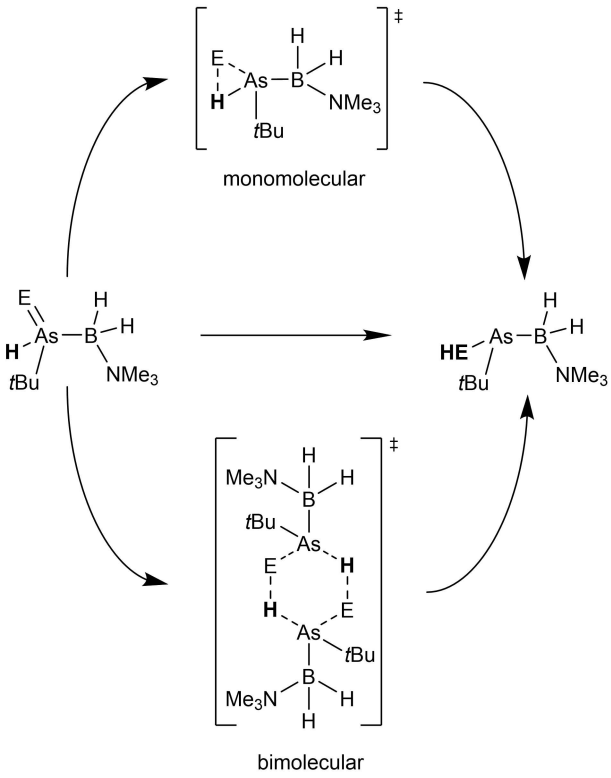

Scheme 8. Simplified isomerization pathways, computationally investigated for the formation of isomers of **2**, **3a** and **6a**.

Research Article
doi.org/10.1002/ejic.202300338

Table 1. Reaction enthalpies ΔH°_{298} and activation enthalpies $\Delta H^{\#}_{298}$ (kJ mol^{-1}) for mono- and bimolecular isomerization pathways.

	monomolecular		bimolecular[a)]	
E	ΔH°_{298}	$\Delta H^{\#}_{298}$	ΔH°_{298}	$\Delta H^{\#}_{298}$
O	−60	185	−131	35
S	−19	172	−31	67
Se	−8	137	+2	79

[a)] values per mol of dimer.

In contrast, the bimolecular pathway is highly exothermic for E = O, exothermic in case of E = S and slightly endothermic in case of E = Se. The activation enthalpies are much smaller, especially in case of E = O. Computational results suggest, that in case of oxygen- and sulfur-containing derivatives, the initial products **3a** and **6a** are expected to intermolecularly isomerize to the according As–E–H isomers **3a'** and **6a'**, while in case of **2** such isomerization is energetically unfavorable and is kinetically hindered.

Our computational findings are in qualitative agreement with experimental observations. In the vibrational spectra of **3a** and **6a** only weak bands for an As–H stretching bond are observed, while peaks for an E–H vibration are clearly visible, indicating a mixture of the two isomers. In the ^{1}H NMR spectra of **3a** and **6a** signals corresponding to a potential E–H group are observed alongside the signals corresponding to the As–H moiety of the As=E isomer. However, in all cases the compounds containing an As–H moiety are the main product, indicating an isomerization in solution over the time. Although not perfectly suited for the detection of H-atoms, the single crystal XRD data indicates a product with an As–H moiety in case of **2**, which is in agreement with the computational findings and the NMR spectroscopic data.

Conclusions

In summary, *t*BuAsHBH$_2$NMe$_3$ (**1**) can serve as a promising starting material for the synthesis of new compounds containing a group 13–15-16 structural motif. The reaction of **1** with grey selenium leads to the selective formation of *t*BuAs(Se)HBH$_2$NMe$_3$ (**2**), which was isolated and fully characterized. The reaction with two equivalents of Se only lead to the decomposition of the starting material. In the case of sulfur, two different compounds *t*BuAs(S)HBH$_2$NMe$_3$ (**3a**) and *t*BuAs(S)SHBH$_2$NMe$_3$ (**3b**) were isolated as oils and completely characterized in solution. However, the characterization in the solid state was not possible, as the compounds reveal rapid decomposition under crystallization conditions despite various attempts to prevent this. Additionally, the larger aggregate (Me$_3$NBH$_2$*t*BuAs(S)S)$_3$As (**4**), a decomposition product of **3a**, could be isolated and structurally characterized by X-ray diffraction analysis and DFT computations. It reveals three moieties of **3b** connected via a central arsenic atom providing valuable information on the decomposition pathway of **3a** and **3b**.

For the reaction of **1** towards oxygen sources such as MesCNO, a novel example of an As–H activation leading to 1-(Me$_3$NBH$_2$*t*BuAs–C-NOH)-2,4,6-methylbenzene (**5**) was observed. Additionally, also the first isolatable oxo-arsanylboranes *t*BuAs(O)HBH$_2$NMe$_3$ (**6a**) and *t*BuAs(O)OHBH$_2$NMe$_3$ (**6b**) could be synthesized and fully characterized. For **6b**, also the X-ray structure in the solid state could be obtained. This is the first ever example of an isolated oxo-arsanylborane in the solid state, making **1** the so far best arsanylborane to build up arsenic-based labile 13–15-16 compounds. This is even more noteworthy as the compounds obtained from the reaction with the oxygen sources **5**, **6a** and **6b** are all very unstable in solution and decompose within short time frames even at low temperatures. A similar decomposition behavior, although at a slower pace, has also been observed for the sulfur compounds **3a** and **3b**.

Additionally, computational studies concerning the tautomers of compounds **2**, **3a** and **6a** have been performed, indicating an intermolecular transformation of the originally formed As–H tautomers to the thermodynamically favored As–E–H isomers **3a'** and **6a'** in case of oxygen and sulfur. These results are additionally supported by spectroscopic data, although no structural proof of these isomers could be obtained.

Experimental Section

Experimental procedures for the synthesis of all compounds, analytical data, quantum chemical calculations and X-ray crystallography are described in the Supporting Information.

Deposition numbers CCDC-2267008 (**2**), CCDC-2267009 (**4**), CCDC-2267010 (**5**), CCDC-2267011 (**6b**), and CCDC-2267012 (**6b x H_2O**) contain the supplementary crystallographic data for this paper. These data are provided free of charge by the joint Cambridge Crystallographic Data Centre and Fachinformationszentrum Karlsruhe Access Structures service.

Acknowledgements

This work was supported by the Deutsche Forschungsgemeinschaft (DFG) within the project Sche 384/41-1. This work was supported by the joint DFG-RSF grant (RSF project 21-43-04404). Use of computational resources of the Research center «Computing Center» of the research park of St. Petersburg State University is acknowledged. Open Access funding enabled and organized by Projekt DEAL.

Conflict of Interests

The authors declare no conflict of interest.

Data Availability Statement

The data that support the findings of this study are available in the supplementary material of this article.

Keywords: Arsenic · Boron · Hydroarsination · Main group · Oxidation

[1] a) J. Linshoeft, E. J. Baum, A. Hussain, P. J. Gates, C. Näther, A. Staubitz, *Angew. Chem. Int. Ed.* **2014**, *53*, 12916–12920; b) A. Hübner, Z.-W. Qu, U. Englert, M. Bolte, H.-W. Lerner, M. C. Holthausen, M. Wagner, *J. Am. Chem. Soc.* **2011**, *133*, 4596–4609; c) R. H. Neilson, P. Wisian-Neilson, *Chem. Rev.* **1988**, *88*, 541–562; d) R. De Jaeger, M. Gleria, *Prog. Polym. Sci.* **1998**, *23*, 179–276; e) M. Liang, I. Manners, *J. Am. Chem. Soc.* **1991**, *113*, 4044–4045; f) A. M. Priegert, B. W. Rawe, S. C. Serin, D. P. Gates, *Chem. Soc. Rev.* **2016**, *45*, 922–953; g) I. Manners, *Angew. Chem. Int. Ed.* **1996**, *35*, 1602–1621; h) R. D. Miller, J. Michl, *Chem. Rev.* **1989**, *89*, 1359–1410; i) F. Choffat, S. Käser, P. Wolfer, D. Schmid, R. Mezzenga, P. Smith, W. Caseri, *Macromolecules* **2007**, *40*, 7878–7889; j) F. Jäkle, *Chem. Rev.* **2010**, *110*, 3985–4022; k) B. W. Rawe, C. P. Chun, D. P. Gates, *Chem. Sci.* **2014**, *5*, 4928–4938; l) X. He, T. Baumgartner, *RSC Adv.* **2013**, *3*, 11334–11350; m) H. R. Allcock, *Chem. Mater.* **1994**, *6*, 1476–1491; n) G. Zhang, G. M. Palmer, M. W. Dewhirst, C. L. Fraser, *Nat. Mater.* **2009**, *8*, 747–751; o) P. J. Fazen, J. S. Beck, A. T. Lynch, E. E. Remsen, L. G. Sneddon, *Chem. Mater.* **1990**, *2*, 96–97; p) R. West, *J. Organomet. Chem.* **1986**, *300*, 327–346; q) F. Vidal, F. Jäkle, *Angew. Chem. Int. Ed.* **2019**, *58*, 5846–5870; r) C. H. Honeyman, I. Manners, C. T. Morrissey, H. R. Allcock, *J. Am. Chem. Soc.* **1995**, *117*, 7035–7036; s) T. Wideman, P. J. Fazen, K. Su, E. E. Remsen, G. A. Zank, L. G. Sneddon, *Appl. Organomet. Chem.* **1998**, *12*, 681–693.

[2] a) A. C. Jones, P. O'Brien, *CVD of compound semiconductors: Precursor synthesis, developmeny and applications*, John Wiley & Sons, **2008**; b) F. C. Sauls, L. V. Interrante, *Coord. Chem. Rev.* **1993**, *128*, 193–207; c) S. Schulz, in *Adv. Organomet. Chem., Vol. 49*, Academic Press, **2003**, pp. 225–317; d) S. Schulz, *Coord. Chem. Rev.* **2001**, *215*, 1–37; e) R. L. Wells, W. L. Gladfelter, *J. Cluster Sci.* **1997**, *8*, 217–238.

[3] a) A. Staubitz, A. P. M. Robertson, M. E. Sloan, I. Manners, *Chem. Rev.* **2010**, *110*, 4023–4078; b) K. Takrouri, V. M. Dembistky, M. Srebnik, in *Studies in Inorganic Chemistry, Vol. 22* (Eds.: H. A. Ali, V. M. Dembitsky, M. Srebnik), Elsevier, **2005**, pp. 495–549; c) B. Carboni, L. Monnier, *Tetrahedron* **1999**, *55*, 1197–1248; d) G. Pawelke, H. Bürger, *Appl. Organomet. Chem.* **1996**, *10*, 147–174; e) J. M. Brunel, B. Faure, M. Maffei, *Coord. Chem. Rev.* **1998**, *178–180*, 665–698.

[4] a) A. Staubitz, A. P. Robertson, I. Manners, *Chem. Rev.* **2010**, *110*, 4079–4124; b) C. W. Hamilton, R. T. Baker, A. Staubitz, I. Manners, *Chem. Soc. Rev.* **2009**, *38*, 279–293; c) F. H. Stephens, V. Pons, R. Tom Baker, *Dalton Trans.* **2007**, 2613–2626; d) A. Gutowska, L. Li, Y. Shin, C. M. Wang, X. S. Li, J. C. Linehan, R. S. Smith, B. D. Kay, B. Schmid, W. Shaw, M. Gutowski, T. Autrey, *Angew. Chem. Int. Ed.* **2005**, *44*, 3578–3582; e) R. J. Keaton, J. M. Blacquiere, R. T. Baker, *J. Am. Chem. Soc.* **2007**, *129*, 1844–1845; f) M. C. Denney, V. Pons, T. J. Hebden, D. M. Heinekey, K. I. Goldberg, *J. Am. Chem. Soc.* **2006**, *128*, 12048–12049; g) Z. Liu, T. B. Marder, *Angew. Chem. Int. Ed.* **2008**, *47*, 242–244; h) V. Pons, R. T. Baker, *Angew. Chem. Int. Ed.* **2008**, *47*, 9600–9602; i) G. Alcaraz, S. Sabo-Etienne, *Angew. Chem. Int. Ed.* **2010**, *49*, 7170–7179; j) M. E. Sloan, A. Staubitz, T. J. Clark, C. A. Russell, G. C. Lloyd-Jones, I. Manners, *J. Am. Chem. Soc.* **2010**, *132*, 3831–3841.

[5] a) C. A. Jaska, K. Temple, A. J. Lough, I. Manners, *J. Am. Chem. Soc.* **2003**, *125*, 9424–9434; b) A. Staubitz, A. Presa Soto, I. Manners, *Angew. Chem. Int. Ed.* **2008**, *47*, 6212–6215; c) J. R. Vance, A. P. Robertson, K. Lee, I. Manners, *Chem. Eur. J.* **2011**, *17*, 4099–4103; d) R. Dallanegra, A. P. Robertson, A. B. Chaplin, I. Manners, A. S. Weller, *Chem. Commun.* **2011**, *47*, 3763–3765; e) A. Staubitz, M. E. Sloan, A. P. M. Robertson, A. Friedrich, S. Schneider, P. J. Gates, J. Schmedt auf der Günne, I. Manners, *J. Am. Chem. Soc.* **2010**, *132*, 13332–13345; f) B. L. Dietrich, K. I. Goldberg, D. M. Heinekey, T. Autrey, J. C. Linehan, *Inorg. Chem.* **2008**, *47*, 8583–8585; g) H. C. Johnson, A. P. Robertson, A. B. Chaplin, L. J. Sewell, A. L. Thompson, M. F. Haddow, I. Manners, A. S. Weller, *J. Am. Chem. Soc.* **2011**, *133*, 11076–11079; h) A. L. Colebatch, A. S. Weller, *Chem. Eur. J.* **2019**, *25*, 1379–1390; i) D. Han, F. Anke, M. Trose, T. Beweries, *Coord. Chem. Rev.* **2019**, *380*, 260–286; j) L. J. Morris, N. A. Rajabi, M. S. Hill, I. Manners, C. L. McMullin, M. F. Mahon, *Dalton Trans.* **2020**, *49*, 14584–14591; k) L. Wirtz, J. Lambert, B. Morgenstern, A. Schäfer, *Organometallics* **2021**, *40*, 2108–2117; l) A. N. Marziale, A. Friedrich, I. Klopsch, M. Drees, V. R. Celinski, J. Schmedt auf der Günne, S. Schneider, *J. Am. Chem. Soc.* **2013**, *135*, 13342–13355; m) H. C. Johnson, E. M. Leitao, G. R. Whittell, I. Manners, G. C. Lloyd-Jones, A. S. Weller, *J. Am. Chem. Soc.* **2014**, *136*, 9078–9093; n) H. C. Johnson, A. S. Weller, *Angew. Chem. Int. Ed.* **2015**, *54*, 10173–10177; o) M. E. Bluhm, M. G. Bradley, R. Butterick, U. Kusari, L. G. Sneddon, *J. Am. Chem. Soc.* **2006**, *128*, 7748–7749.

[6] a) D. W. Himmelberger, C. W. Yoon, M. E. Bluhm, P. J. Carroll, L. G. Sneddon, *J. Am. Chem. Soc.* **2009**, *131*, 14101–14110; b) H. Dorn, R. A. Singh, J. A. Massey, J. M. Nelson, C. A. Jaska, A. J. Lough, I. Manners, *J. Am. Chem. Soc.* **2000**, *122*, 6669–6678; c) H. Dorn, J. M. Rodezno, B. Brunnhöfer, E. Rivard, J. A. Massey, I. Manners, *Macromolecules* **2003**, *36*, 291–297; d) T. J. Clark, J. M. Rodezno, S. B. Clendenning, S. Aouba, P. M. Brodersen, A. J. Lough, H. E. Ruda, I. Manners, *Chem. Eur. J.* **2005**, *11*, 4526–4534; e) S. Pandey, P. Lönnecke, E. Hey-Hawkins, *Eur. J. Inorg. Chem.* **2014**, *14*, 2456–2465; f) D. Jacquemin, C. Lambert, E. A. Perpète, *Macromolecules* **2004**, *37*, 1009–1015; g) A. Schäfer, T. Jurca, J. Turner, J. R. Vance, K. Lee, V. A. Du, M. F. Haddow, G. R. Whittell, I. Manners, *Angew. Chem. Int. Ed.* **2015**, *54*, 4836–4841; h) J.-M. Denis, H. Forintos, H. Szelke, L. Toupet, T.-N. Pham, P.-J. Madec, A.-C. Gaumont, *Chem. Commun.* **2003**, 54–55; i) H. Dorn, R. A. Singh, J. A. Massey, A. J. Lough, I. Manners, *Angew. Chem. Int. Ed.* **1999**, *38*, 3321–3323; j) M. A. Huertos, A. S. Weller, *Chem. Commun.* **2012**, *48*, 7185–7187; k) M. A. Huertos, A. S. Weller, *Chem. Sci.* **2013**, *4*, 1881–1888; l) T. N. Hooper, M. A. Huertos, T. Jurca, S. D. Pike, A. S. Weller, I. Manners, *Inorg. Chem.* **2014**, *53*, 3716–3729; m) L. Barton, O. Volkov, M. Hata, P. McQuade, N. P. Rath, *Pure Appl. Chem.* **2003**, *75*, 1165–1173; n) H. Schmidbaur, *J. Organomet. Chem.* **1980**, *200*, 287–306.

[7] a) R. Woods-Robinson, Y. Han, H. Zhang, T. Ablekim, I. Khan, K. A. Persson, A. Zakutayev, *Chem. Rev.* **2020**, *120*, 4007–4055; b) L. Zhang, S. M. Fakhouri, F. Liu, J. C. Timmons, N. A. Ran, A. L. Briseno, *J. Mater. Chem.* **2011**, *21*, 1329–1337; c) M. Jeffries-El, B. M. Kobilka, B. J. Hale, *Macromolecules* **2014**, *47*, 7253–7271; d) R. L. Brutchey, *Acc. Chem. Res.* **2015**, *48*, 2918–2926; e) N. Tohge, T. Minami, M. Tanaka, *J. Non-Cryst. Solids* **1980**, *37*, 23–30; f) J. Zhou, G.-Q. Bian, Q.-Y. Zhu, Y. Zhang, C.-Y. Li, J. Dai, *J. Solid State Chem.* **2009**, *182*, 259–264; g) M. Huang, P. Xu, D. Han, J. Tang, S. Chen, *ACS Appl. Mater. Interfaces* **2019**, *11*, 15564–15572.

[8] a) M. Brynda, *Coord. Chem. Rev.* **2005**, *249*, 2013–2034; b) F. Uhlig, E. Herrmann, D. Schädler, G. Ohms, G. Großmann, S. Besser, R. Herbst-Irmer, *Z. Anorg. Allg. Chem.* **1993**, *619*, 1962–1970.

[9] a) M. Jesberger, T. P. Davis, L. Barner, *Synthesis* **2003**, *2003*, 1929–1958; b) M. St. John Foreman, J. D. Woollins, *Dalton Trans.* **2000**, 1533–1543; c) M. P. Cava, M. I. Levinson, *Tetrahedron* **1985**, *41*, 5061–5087; d) R. A. Cherkasov, G. A. Kutyrev, A. N. Pudovik, *Tetrahedron* **1985**, *41*, 2567–2624.

[10] a) J. D. Woollins, *Synlett* **2012**, *2012*, 1154–1169; b) G. Hua, J. D. Woollins, in *Selenium and Telurium Chemistry*, Vol, 1 (Eds: J.Woollins, R. Laitinen), Springer, Berlin, Heidelberg, **2011**, pp. 1–39; c) L. Ascherl, A. Nordheider, K. S. A. Arachchige, D. B. Cordes, K. Karaghiosoff, M. Bühl, A. M. Z. Slawin, J. D. Woollins, *Chem. Commun.* **2014**, *50*, 6214–6216.

[11] R. Davies, L. Patel, in *Handbook of chalcogen chemistry: new perspectives in sulfur, selenium and tellurium, Vol, 1* (Eds: F. Devillanova, W.-W. Laitinen), *RSC*, Cambridge, **2013**, 238–306.

[12] a) B. Wrackmeyer, E. V. Klimkina, W. Milius, *Eur. J. Inorg. Chem.* **2014**, *2014*, 4865–4876; b) B. Bildstein, F. Sladky, *Phosphorus Sulfur Silicon Relat. Elem.* **1990**, *47*, 341–347; c) F. Dornhaus, M. Bolte, H.-W. Lerner, M. Wagner, *Eur. J. Inorg. Chem.* **2006**, *2006*, 5138–5147.

[13] a) K.-C. Schwan, A. Y. Timoskin, M. Zabel, M. Scheer, *Chem. Eur. J.* **2006**, *12*, 4900–4908; b) C. Marquardt, O. Hegen, T. Kahoun, M. Scheer, *Chem. Eur. J.* **2017**, *23*, 4397–4404.

[14] a) R. F. de Ketelaere, F. T. Delbeke, G. P. Van Der Kelen, *J. Organomet. Chem.* **1971**, *28*, 217–223; b) A. Merijanian, R. A. Zingaro, *Inorg. Chem.* **1966**, *5*, 187–191.

[15] a) V. Krishnan, A. Datta, S. V. L. Narayana, *J. Inorg. Nucl. Chem.* **1977**, *13*, 517–522; b) S. V. L. Narayana, H. N. Shrivastava, *Acta Crystallogr. Sect. B* **1981**, *37*, 1186–1189; c) D. H. Brown, A. F. Cameron, R. J. Cross, M. McLaren, *Dalton Trans.* **1981**, 1459–1462; d) G. Sakane, T. Shibahara, H. Hou, Y. Liu, X. Xin, *Transition Met. Chem.* **1996**, *21*, 398–400.

[16] O. Hegen, A. V. Virovets, A. Y. Timoshkin, M. Scheer, *Chem. Eur. J.* **2018**, *24*, 16521–16525.

[17] F. Lehnfeld, M. Seidl, A. Y. Timoshkin, M. Scheer, *Eur. J. Inorg. Chem.* **2022**, *2022*, e202100930.

[18] C. Marquardt, A. Adolf, A. Stauber, M. Bodensteiner, A. V. Virovets, A. Y. Timoshkin, M. Scheer, *Chem. Eur. J.* **2013**, *19*, 11887–11891.

Manuscript received: June 1, 2023
Revised manuscript received: July 11, 2023
Accepted manuscript online: July 12, 2023
Version of record online: ■■, ■■

RESEARCH ARTICLE

The controlled oxidation of the LB-stabilized arsanylborane *t*BuAsHBH$_2$NMe$_3$ with the chalcogenes Se and S_8 and the oxidants mesitylnitrile-N-oxide and trimethylamine-N-oxide is reported. In addition to novel mixed group 13–15-16 compounds including the first isolable oxo-arsanylborane, also a hydroarsination reaction occurs.

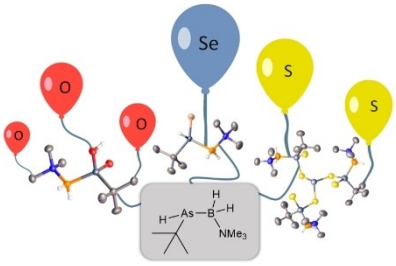

*Dr. F. Lehnfeld, Dr. M. Seidl, Prof. Dr. A. Y. Timoshkin, Prof. Dr. M. Scheer**